The accuracy of the velocity approximation with respect to the pressure approximation for incompressible fluid flow.

Gunnar A. Staff and Kent-Andre Mardal

Simula Research Laboratory

Abstract

We consider the accuracy of the velocity approximation with respect to the pressure approximation using various standard finite element methods for incompressible fluid flow. Of particular interest is the case where the hydrostatic part of the pressure is dominating, which implies that the pressure may be large relative to the velocity. Some standard mixed elements like the Mini element and the Taylor-Hood element handle this case well, while others like the $P_2 - P_0$ element and the Crouzeix-Raviart element do not. This seems to be related to the fact that the Taylor-Hood and the Mini elements yield a stable approximation of the mixed Poisson problem.

Key words: Navier-Stokes, mixed finite elements, characteristic scales, mass conservation, inf-sup condition

INTRODUCTION

In this paper we consider the motion of an incompressible fluid in the case where the pressure is dominated by a hydrostatic part. This means that there are two natural characteristic scales present in the physical problem; the scale induced by the (hydrostatic) pressure and the scale naturally induced by the velocity. These scales may differ by several orders of magnitude. Earlier we have encountered this problem in simulation of the movements of the continental plates where the characteristic scales of the velocity and the pressure differ with at least four orders of magnitude. We will study how various finite elements handle this situation, both by a theoretical and a numerical approach.

To analyze the situation we introduce a Stokes problem on the following form,

$$
\begin{aligned}
-\Delta \mathbf{u} + \nabla p &= \nabla g + \epsilon \mathbf{f}, \quad \text{in } \Omega, && (1)\\
\nabla \cdot \mathbf{u} &= 0, \quad \text{in } \Omega, && (2)\\
\mathbf{u} &= 0, \quad \text{on } \partial\Omega, && (3)
\end{aligned}
$$

where ϵ is a small number, $\mathbf{u}$ and p are the velocity and pressure of the fluid, respectively, $\nabla g + \epsilon \mathbf{f}$ is the body force, and $\Delta = \nabla^2$ is the Laplacian operator. As we will describe later, ∇g typically represents the gravity, while $\epsilon \mathbf{f}$ represents other forces. The solutions $\mathbf{u}$ and p of the above equations may be very differently scaled if ϵ is small. As $\epsilon \to 0$, $p \to g$ and $\mathbf{u} \to 0$. In the limit case where $\epsilon = 0$ we obtain the equation for the hydrostatic pressure. We remark that neither g nor ∇g need to be explicitly constructed, $\nabla g + \epsilon \mathbf{f}$ is only a representation useful for the theoretical purposes, i.e., it is not necessary to compute the hydrostatic pressure, which as we will see later would involve the solution of a Poisson problem. Later we generalize our observations to the stationary Navier-Stokes equations with more general boundary conditions.

As a tool to discretize in space, we choose the finite element method. This is due to the strong theoretical foundation of the method, which will be used to derive improved theoretical error estimates for problems on the form (1)-(2). However, it is also due to the fact that finite element methods are a mature method, with an increasing popularity in real applications. Standard error estimates state that the errors of the pressure and the velocity influence each other. In particular this means that a small relative error in the pressure may contribute significantly

to the velocity error when the characteristic scales are very different. We will describe this in more detail later.

Several methods conserve the mass exactly, and give an error estimate for the velocity which is independent of the error in the pressure approximation (Girault and Raviar, 1986; Gunzburger, 1989; Turek, 1999). However, these methods are impractical and much less used than standard finite elements. It seems natural to assume that the next best thing after exact mass conservation is element-wise mass conservation. Many elements have this property, e.g the $P_2 - P_0$ (continuous quadratic polynomials for the velocity and piecewise constant functions for the pressure), the non-conforming Crouzeix-Raviart element (Crouzeix and Raviart, 1973) and the corresponding Rannacher-Turek elements (Rannacher and Turek, 1992). However, it is not clear that element-wise mass conservation actually improves the velocity approximation. In fact, in this work we show that elements with continuous pressure, and only global mass conservation, such as the Mini element (Arnold et al., 1984) and the Taylor-Hood element are superior to the elements with element-wise mass conservation, in the case with two different scales.

An outline of the paper is as follows. In the next section, a small example is presented to illustrate the different behavior of two standard elements like the Taylor-Hood, and the $P_2 - P_0$ element. The following section motivates our work by reviewing why the gravity is a gradient and presenting a method for removing the hydrostatic pressure from the Stokes equation. The next section presents some difficulties when the model problem is discretized. It also motivates that the ability to solve the mixed Poisson problem is an important property in this two scale problem. The two last sections present numerical experiments. First we solve the Stokes problem by using the Mini element, the Crouzeix-Raviart element and a stabilized linear element. Then we solve the stationary Navier-Stokes with general boundary conditions using the Taylor-Hood element and the $P_2 - P_0$ element.

AN ILLUSTRATIVE EXAMPLE WITH VARIABLE DENSITY

A simple problem with variable density is depictured in Figure 1. The problem is modelled as,

$$-\mu\Delta\mathbf{u} + \nabla p = \rho\mathbf{G}_0, \text{ in } \Omega = (0,1)\times(0,1), \tag{4}$$

$$\nabla\cdot\mathbf{u} = 0, \text{ in } \Omega, \tag{5}$$

$$\mathbf{u} = 0, \text{ on } \partial\Omega \tag{6}$$

where $\mathbf{G}_0 = \begin{bmatrix} 0 \\ G_0 \end{bmatrix}$, G_0 is the acceleration of the gravity, and the ρ is the density.

The interface between the two fluids with different densities is given with an angle θ with respect to the x-axis as illustrated in Figure 1. If the fluid with the largest density is on top, the problem is unstable. This is the case for tectonic plates, which are slightly denser than the mantel. For simplicity, and with no loss in generality, we assume that the viscosity is constant. Physical reasoning says that for small values of θ, the velocity is small. This means that for increasing density, the pressure has to be equal to the greater part of the increasing body force.

Since we argue that this problem suffers from very different characteristic scales for the pressure and the velocity, which again leads to a numerical breakdown for some standard mixed elements, we need to show that scaling does not elimiate the difference in the characteristic scales.

The following scales are chosen:

$$\bar{\mathbf{u}} = \frac{\mathbf{u}}{U},\ \bar{x_i} = \frac{x_i}{L},\ \bar{\rho} = \frac{\rho}{\rho_0},\ \bar{\mu} = \frac{\mu}{\mu_0} = 1,\ \bar{p} = \frac{p}{P}.$$

By inserting this into (4) and dividing the constants in front of the pressure, we get

$$-\frac{\mu_0 U}{PL}\Delta\bar{\mathbf{u}} + \nabla\bar{p} = \frac{\rho_0 L}{P}\bar{\rho}\mathbf{G}_0.$$

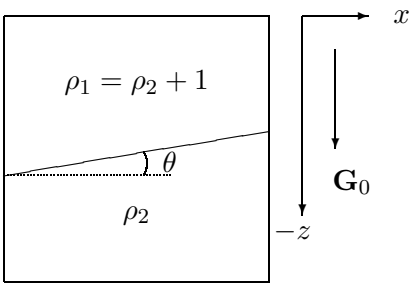

Fig. 1: A simple box problem with variable density. The gravity force is directed downwards parallel to the z-axis. The interface between the two fluids is rotated with an angle θ with respect to the x-axis. The relative difference between the densities is always one, and the fluid with the highest density is always on the top.

We will now present two possible scalings, and show that both of them end up with a problem where the characteristic scales of the velocity and pressure are very different.

First we assume that we can find U, and choose the standard pressure scaling for viscous flow, i.e. $P = \frac{\mu_0 U}{L}$. The scaled equation is then

$$-\Delta \bar{\mathbf{u}} + \nabla \bar{p} = \frac{\rho_0 L^2}{\mu_0 U} \bar{\rho} \mathbf{G}_0. \tag{7}$$

Lets assume that the realtive difference between the densities is fixed, $\rho_1 - \rho_2 = 1$, while the absolute values vary, $\rho_2 = 1, 100, 10000$. For small values of θ, it is physically reasonable to assume that the velocity is small. If $\rho_0 \gg \mu_0$, then $\frac{\rho_0 L^2}{\mu_0 U} \gg 1$. This gets worse for larger values of ρ_0. By assuming that $\rho_0 = \rho_1$ from our example,

$$\bar{\rho} = \begin{cases} 1, & \text{in part 1} \\ 1 - \varepsilon, & \text{in part 2,} \end{cases}$$

where $\varepsilon = \frac{1}{\rho_1}$. The variation in $\bar{\rho}$ decreases as ρ increases. Assuming ρ is large, we clearly have two different scales in the problem since the velocity stays small, while the pressure has to be equal to the greater part of the body force.

One could think of removing the large right-hand side by a rescaling according to

$$P = \rho_0 G_0 L, \quad U = \frac{PL}{\mu_0} = \frac{\rho_0 G_0 L^2}{\mu_0},$$

where the equation now is seemingly well scaled:

$$-\Delta \bar{\mathbf{u}} + \nabla \bar{p} = \bar{\rho} = 1 - \varepsilon, \quad \varepsilon = \frac{1}{\rho_0}.$$

However, by looking at the scale factor for the velocity, $U = \frac{\rho_0 G_0 L^2}{\mu_0}$, we notice that it is increasing linearly with ρ_0. We know from physical reasoning that the velocity is relatively small, and thus the velocity scaling is bad for large values of ρ.

We now present results based on simulation of (7), but simulations of the second scaling approach gives the same conclusion. The angle θ is set to five degrees. The simulations are done with the same number of elements for the different values of ρ, but the discretization using the $P_2 - P_0$ element uses about 5 times as many elements as the Taylor-Hood discretization. This is to magnify the different approximation properties of these two elements for this particular problem. Figure 2 and 3 show the pressure and velocity fields computed with the Taylor-Hood element. As expected this scaling gives a constant velocity for increasing ρ while the pressure is increasing.

On the other hand, the velocity field computed by the $P_2 - P_0$ element, shown in Figure 4, does not look physical for high values of ρ. This is even though this simulation uses about five times as many elements as the the simulation using the Taylor-Hood element. The velocity field appears to be oscillating badly. Furthermore, the velocity is totally out of scale. In the leftmost picture $\|\mathbf{u}\|_\infty \approx 1.3 \cdot 10^{-3}$, which is roughly correct, in the middle picture $\|\mathbf{u}\|_\infty \approx 2.9 \cdot 10^{-3}$ and in rightmost picture $\|\mathbf{u}\|_\infty \approx 1.8 \cdot 10^{-1}$. Notice further that similar experiments with the Mini element give results that are similar to the case with the Taylor–Hood element, while similar experiments with the Crouzeix-Raviart element give results that are similar to the case with the $P_2 - P_0$ element. Hence, it seems that elements with continuous pressure handle the situation well, in contrast to those with discontinuous pressure which suffer from a severe break-down. Why this is the case, and what kind of error estimates we can expect from the elements that work, is what we intend to investigate in the following sections.

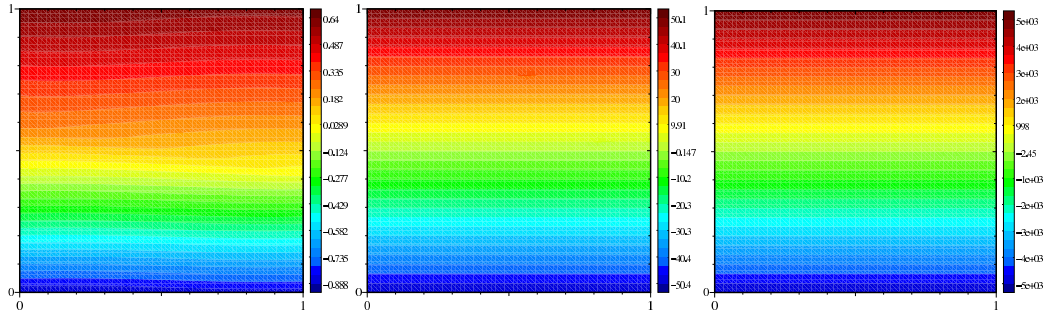

Fig. 2: Plot of the pressure field using the Taylor-Hood element. From left to right we have $\rho_2 = \{1, 100, 10000\}$. The results are correct in the eye-norm for all the configurations of ρ. This is as expected.

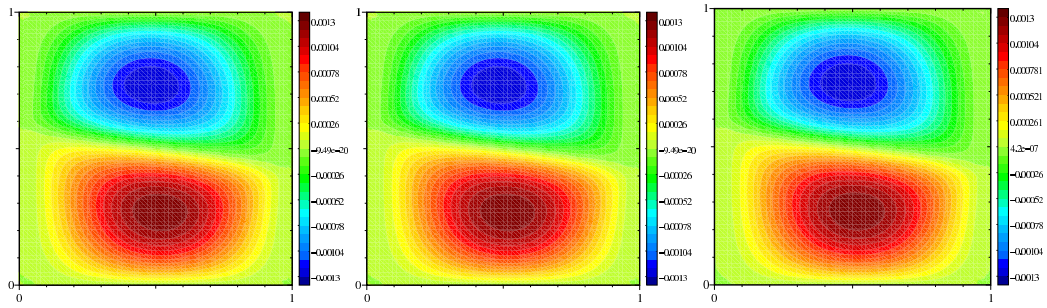

Fig. 3: Plot of the velocity field in the x-direction using the Taylor-Hood element. From left to right we have $\rho_2 = \{1, 100, 10000\}$. The results are correct in the eye-norm for all the configurations of ρ. This is as expected.

Finally, we remark that it is possible to remove the hydrostatic pressure. We write (4)-(6) as

$$\begin{aligned} -\mu\Delta\mathbf{u} + \nabla p_1 &= \rho G_0 - \nabla p_2 \quad \text{in } \Omega = (0,1)\times(0,1) \\ \nabla\cdot\mathbf{u} &= 0 \quad \text{in } \Omega \\ \mathbf{u} &= 0 \quad \text{on } \partial\Omega, \end{aligned}$$

and let p_2 be the solution in the fluid at rest with $\rho = \rho_2$. Then $p_2 = \rho_2 G_0 z$. The right hand side will then be

$$\rho\mathbf{G}_0 - \nabla p_2 = \rho \begin{bmatrix} 0 \\ G_0 \end{bmatrix} - \rho_2 \begin{bmatrix} 0 \\ G_0 \end{bmatrix} = \begin{cases} \mathbf{G}_0, & \text{if } \rho = \rho_1 \\ 0, & \text{if } \rho = \rho_2 \end{cases}.$$

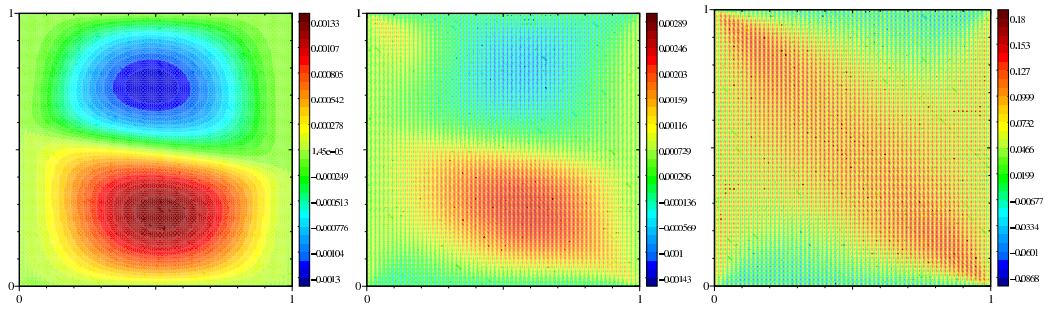

Fig. 4: Plot of the velocity field in the x-direction using the $P_2 - P_0$ element. From left to right we have $\rho_1 = \{1, 100, 10000\}$. In the left picture ($\rho_1 = 2, \rho_2 = 1$), the result are correct in the eye-norm. In the middle plot ($\rho_1 = 101,\ \rho_2 = 100$), the result is polluted by oscillations. The rightmost plot is even worse.

Hence, by removing the hydrostatic part of the pressure, the model problem is nicely scaled. This is the idea we explore in this paper, and in fact it seems that some methods, like the Taylor-Hood and the Mini element automatically remove this part. Hence, it is not necessary to compute the hydrostatic pressure, which in general involves the solution of another PDE problem.

STABILITY IN THE CONTINUOUS CASE FOR THE STOKES PROBLEM

We will now describe the gravity force, the hydrostatic pressure approximation, and the reason for analyzing the problem on the form (1)-(3). In cases with variable density, the gravitational force is not a constant. However, from potential theory (Lin and Segel, 1974), we know that the gravitational force can be computed by solving the following Poisson equation for the gravitational potential g,

$$-\Delta g = 4\pi\rho, \quad \text{in } \Omega$$

where ρ is the density, and suitable boundary conditions are

$$\frac{\partial g}{\partial \mathbf{n}} = \mathbf{G}_0 \cdot \mathbf{n}, \quad \text{on } \partial\Omega$$

where $\mathbf{G}_0$ is the gravitational force on $\partial\Omega$. The corresponding gravitational force $\mathbf{G}$ is

$$\mathbf{G} = \nabla g, \quad \text{in } \Omega$$

Hence, gravity is always a gradient (Lin and Segel, 1974). In contrast the Dirichlet boundary conditions have to obey the divergence constraint and is therefore a curl. Hence, one can think of ∇g as representing the gravity force, while $\epsilon\mathbf{f}$ is the boundary conditions (at least if one use the standard trick to reduce inhomogeneous Dirichlet boundary conditions to homogeneous boundary conditions by modifying the right hand side). In the case of Neumann boundary conditions, both scales will be represented.

We may utilize the fact that the gravity is a gradient by rewriting the Stokes problem. Letting $p = p_1 + p_2$ we may rewrite (1)-(3) as

$$-\Delta\mathbf{u} + \nabla p_1 = \epsilon\mathbf{f} + \nabla g - \nabla p_2, \quad \text{in } \Omega, \tag{8}$$

$$\nabla \cdot \mathbf{u} = 0, \quad \text{in } \Omega, \tag{9}$$

$$\mathbf{u} = 0, \quad \text{on } \partial\Omega. \tag{10}$$

It remains to construct p_2 such that $\nabla g - \nabla p_2$ is small, assuming that ϵ is small. This can be achieved by solving the following Poisson problem, where p_2 balance the right hand side from

(1) (remember that we assume $\epsilon\mathbf{f}$ to be small):

$$\begin{aligned} \Delta p_2 &= \nabla \cdot (\epsilon\mathbf{f} + \nabla g), \\ \frac{\partial p_2}{\partial \mathbf{n}} &= (\epsilon\mathbf{f} + \nabla g) \cdot \mathbf{n} \end{aligned} \tag{11}$$

This Poisson problem can also be written on mixed form (which is the form we will use later):

$$\mathbf{w} + \nabla p_2 = \epsilon\mathbf{f} + \nabla g, \quad \text{in } \Omega, \tag{12}$$

$$\nabla \cdot \mathbf{w} = 0, \quad \text{in } \Omega, \tag{13}$$

$$\mathbf{w} \cdot \mathbf{n} = 0, \quad \text{on } \partial\Omega, \tag{14}$$

Hence, p_2 may be thought of as a generalization of the hydrostatic pressure because $\epsilon \to 0 \Rightarrow \mathbf{w} \to 0$. Since, $\mathbf{w} = \epsilon\mathbf{f} + \nabla g - \nabla p_2$ we end up with,

$$-\Delta\mathbf{u} + \nabla p_1 = \mathbf{w}, \quad \text{in } \Omega, \tag{15}$$

$$\nabla \cdot \mathbf{u} = 0, \quad \text{in } \Omega, \tag{16}$$

$$\mathbf{u} = 0, \quad \text{on } \partial\Omega. \tag{17}$$

One computational approach would be to solve (11) using standard methods, and finding $\mathbf{w}$ using numerical derivation, or (12)-(14) for $\mathbf{w}$ and p_2, using a suitable method for a mixed Poisson problem (e.g. using the Raviart Thomas element). Then we solve (15)-(17) for $\mathbf{u}$ and p_1, using a suitable method for the Stokes problem (e.g. using the Crouzeix-Raviart element). The disadvantage is that we have to solve two PDE problems instead of one.

We would like to remark that the splitting is only an analytically tool to predict how standard elements will approximate (1)-(3). Furthermore, it should be mentioned that in the above analysis we have assumed that ∇g and/or the hydrostatic pressure are not known. If these are known it is natural to remove the hydrostatic part of the pressure before scaling. However, as we will show in the next sections, some standard mixed elements remove this automatically.

STABILITY IN THE DISCRETE CASE FOR THE STOKES PROBLEM

As previously mentioned, we will use standard mixed finite elements to approximate the Stokes problem (1)-(3). Assume now that we want to find the solution $(\mathbf{u}_h, p_h) \in \mathbf{V}_h \times Q_h \subset \mathbf{H}_0^1 \times L_0^2$ where H^n denotes the scalar Sobolev space with n derivatives in L^2, with the associated norm $\|\cdot\|_n$. H_0^n denotes the closure of C_0^∞ in H^n. L_0^2 denotes the set of L^2 functions with the mean value equal to zero. Bold face symbols means the same spaces applied to vectors.

It is well known that a solution method for the Stokes problem must satisfy the inf-sup condition

$$\inf_{q_h \in Q_h} \sup_{\mathbf{u}_h \in \mathbf{V}_h} \frac{(\nabla \cdot \mathbf{u}_h, q_h)}{\|\mathbf{u}_h\|_1} \geq \beta \|q_h\|_0, \tag{18}$$

also known as the Babuska-Brezzi condition. There exist a variety of different mixed elements that satisfy (18). We mention the mixed elements named Mini, Crouzeix-Raviart, $P_2 - P_0$ and Taylor Hood. There also exist stabilization methods that satisfy a modified version of (18). For a thorough introduction to this these elements and other stabilization methods, the reader is referred to (Braess, 2001; Brenner and Scott, 1994; Brezzi and Fortin, 1991; Girault and Raviar, 1986).

By looking at the standard spatial error estimates which are typically on the form

$$\|\mathbf{u} - \mathbf{u}_h\|_1 + \|p - p_h\|_0 \leq Ch^s(\|\mathbf{u}\|_{s+1} + \|p\|_s) \leq \hat{C}h^s\|\epsilon\mathbf{f} + \nabla g\|_{s-1}, \tag{19}$$

where s is the minimum of the order of the element, and the regularity of the solution, we notice that a large p typically results in bad approximation of $\mathbf{u}$ when the characteristic scale

of p is much larger than the characteristic scale of $\mathbf{u}$. Note that this estimate is only true if we have sufficient regularity on the domain and on the right hand side (Bacuta and Bramble, 2003). From our specific right hand side we notice that when ϵ is small, the errors of both the velocity and the pressure are dominated by ∇g.

There exist elements that satisfy the incompressibility constraint exactly, as mentioned in (Girault and Raviar, 1986; Gunzburger, 1989; Turek, 1999) and the references therein. This property ensures that the velocity approximation decouples from the pressure approximation, i.e.,

$$\|\mathbf{u} - \mathbf{u}_h\|_1 \leq Ch^s \|\mathbf{u}\|_{s+1}$$

Another way of ensuring that the velocity and pressure error estimates are decoupled, for conforming methods, is to construct the pressure space such that it is equal to the divergence of the velocity space. Notice however that nonconforming methods additionally need a consistency error independent of p. To the authors knowledge the only finite element having these properties is the element introduced in (Mardal et al., 2002), which is stable for both the Stokes and the mixed Poisson equation.

We will now argue that for some mixed finite elements, the standard error estimate (19) is to pessimistic for (1)-(3). In the previous section we argued that (1)-(3) could be splitted into a coupled mixed Poisson problem (12)-(14) and a Stokes problem (15)-(17). By solving (1)-(3), we in some sense implicitly solve (12)-(14) and (15)-(17). When the hydrostatic part of the pressure is dominating, the error from the mixed Poisson problem will be dominating the error in the velocity. This motivates us to choose elements that also approximate the mixed Poisson problem well.

It is a common misunderstanding that all the standard mixed Stokes elements are not suitable for the mixed Poisson problem. The reason for this misunderstanding is probably the fact that there exist two different formulations of the mixed Poisson problem, and therefore also two so called inf-sup conditions

$$\inf_{q_h \in Q_h} \sup_{\mathbf{v}_h \in \mathbf{V}_h} \frac{(\nabla \cdot \mathbf{v}_h, q_h)}{\|\mathbf{v}_h\|_{\mathbf{H}(\text{div})}} \geq \beta \|q_h\|_0, \qquad \text{for } (\mathbf{w}_h, p_h) \in \mathbf{V}_h \times Q_h \subset \mathbf{H}(\text{div}) \times L^2, \tag{20}$$

$$\inf_{q_h \in Q_h} \sup_{\mathbf{v}_h \in \mathbf{V}_h} \frac{(\nabla \cdot \mathbf{v}_h, q_h)}{\|\mathbf{v}_h\|_0} \geq \beta \|q_h\|_1, \qquad \text{for } (\mathbf{w}_h, p_h) \in \mathbf{V}_h \times Q_h \subset \mathbf{L}^2 \times H^1. \tag{21}$$

We remark that the only differences between inf-sup condition of the Stokes problem (18) and the two alternative inf-sup conditions for the mixed Poisson problem (20) and (21) are the norms on $\mathbf{v}_h$ and q_h. The first (and usual) inf-sup condition (20) is the condition the method should satisfy if the solution is to be found in the $\mathbf{H}(\text{div}) \times L^2$ space. By approximating the solution in $\mathbf{H}(\text{div}) \times L^2$, all the derivatives have to be moved to the velocity and the test function from the velocity approximation space (in the weak form). This is the most commonly used formulation of the mixed Poisson problem, since it gives the highest accuracy on the variable at interest, $\mathbf{w}_h$. None of the standard mixed elements like Mini, Crouzeix-Raviart, Taylor-Hood or $P_2 - P_0$ are stable for the mixed Poisson problem in this approximation space.

On the other hand, the second formulation of the weak inf-sup condition (21) is the stability requirement for a method approximating the mixed Poisson problem in the $\mathbf{L}^2 \times H^1$ space. By approximating the solution in $\mathbf{L}^2 \times H^1$, all the derivatives have to be moved to the pressure and the test function from the pressure approximation space (in the weak form). This weak inf-sup condition is valid for the Taylor-Hood element as shown in (Bercovier and Pironneau, 1979) and the Mini element as shown in (Mardal and Winther, 2004). The terms velocity and pressure in the mixed Poisson problem reflects the terms used for the Stokes problem.

The Crouzeix-Raviart and the $P_2 - P_0$ elements are not stable for the mixed Poisson problem. From this we would expect that the Mini and the Taylor-Hood element will approximate (1)-(3) much better than the Crouzeix-Raviart and the $P_2 - P_0$ element. In the next sections we

present two conjectures that state these improved error estimates, and we will support them by numerical examples.

NUMERICAL EXPERIMENTS ON A STEADY STOKES PROBLEM

In order to validate the new error estimates, we need to compute an example where we have a good measure of the error. This is done by choosing a simple example with a known analytical solution. The problem is given on the domain $\Omega = (0,1) \times (0,1)$, with the exact solution

$$\begin{aligned} \phi &= \epsilon \cos(\pi x) \cos(\pi y), \\ \mathbf{u} &= \nabla \times \phi, \\ p &= \cos(\pi x y) e^{-x} y. \end{aligned} \tag{22}$$

The right hand side is then

$$\epsilon \mathbf{f} + \nabla g = -\Delta \mathbf{u} + \nabla p.$$

By using the standard error estimate (19) we predict that for small values of ϵ the error from the approximation of the pressure may influence the error of the approximation of the velocity, dependent of the choice of element.

We will compare Mini, Crouzeix-Raviart, and stabilized linear elements, which all are a second order approximation of the velocity, when the error is measured in the $\mathbf{L}^2$-norm. The stabilization scheme chosen is

$$\nabla \cdot \mathbf{u} = \beta h^2 \Delta p \tag{23}$$

for the continuity equation, where $\beta = \frac{1}{80}$ corresponds to the Mini element (Section 3.13.3 in (Gresho and Sani, 1998)).

If the analysis from the section discussing the stability of the continuous case is extended into the discrete case, it seems possible to derive an error estimate for the Mini element that takes into account the body forces of our Stokes problem (1)-(3). This is work in progress. Since we will not present the derivation here, the results are presented as a Conjecture based on the numerical experiments.

Conjecture 1 *Assume that we want to solve* (1)-(2) *using the Mini element. Then the error estimates for the velocity can be expressed as*

$$\|\mathbf{u} - \mathbf{u}_h\|_1 \leq C(h\epsilon\|\mathbf{f}\|_0 + h^3\|\epsilon\mathbf{f} + \nabla g\|_0) \tag{24}$$

$$\|\mathbf{u} - \mathbf{u}_h\|_0 \leq C(h^2\epsilon\|\mathbf{f}\|_0 + h^4\|\epsilon\mathbf{f} + \nabla g\|_0)) \tag{25}$$

In contradiction to the standard error estimate, which bounds the sum of the velocity error, and the pressure error, we have presented them separately. This is to make the etismates easier to read. We will first comment the $\mathbf{H}^1$ error of the velocity. If ϵ is large, the term $h\epsilon\|\mathbf{f}\|_0$ is dominating. Notice that contrary to the standard error estimate (19), the error is now bounded by only $\epsilon\|\mathbf{f}\|_0$, instead of $\|\epsilon\mathbf{f} + \nabla g\|_0$. When ϵ decreases (the element size h is kept constant), this will lead to a significantly improved error estimate. The error estimate for the velocity is actually converging linearly with ϵ. When ϵ reaches a given level, $h^3\|\epsilon\mathbf{f} + \nabla g\|_0$ will be dominating. We will now loose our linear convergence with respect to ϵ. But now the convergence is of order three with respect to the element size h, instead of the expected first order. This is also a significant improvement to the standard error estimate (19). The $\mathbf{L}^2$ error estimate is one order higher with respect to the element size h, as expected.

The errors are plotted as a function of ϵ, to illustrate the linear convergence with respect to ϵ for ϵ in a given interval. The different curves in each plot represents different spatial discretization (the number of elements is doubled for each curve).

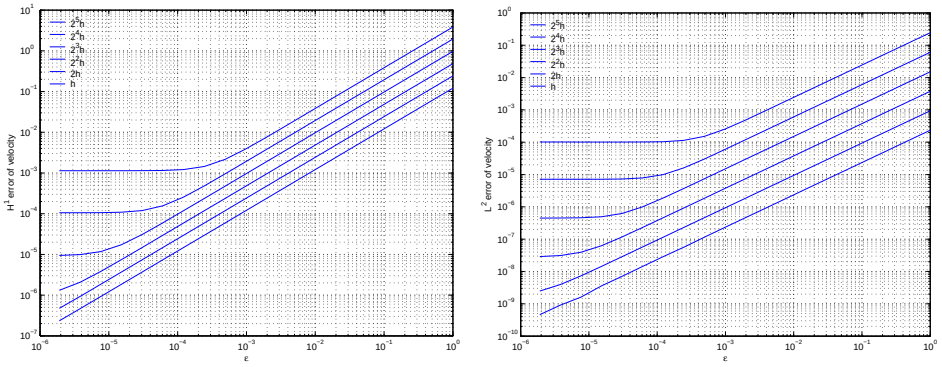

(a) H^1 error of the velocity

(b) L^2 error of the velocity

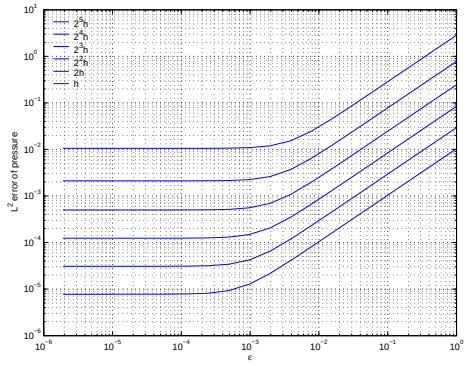

(c) L^2 error of the pressure

Fig. 5: The Mini element applied to out test problem (1)-(3). Convergence results are listed in Table 1. Note the linear convergence with respect to ϵ. This convergence stops when $h\epsilon\|\mathbf{f}\|_0$ is of the the same order of $h^3\|\epsilon\mathbf{f} + \nabla g\|_0$ (for the $\mathbf{H}^1$ error of the velocity), but then we get an increase in the order of convergence with respect to the element size h.

	$\epsilon = 1$	$\epsilon = 2 \cdot 10^{-6}$
$\|\mathbf{u}\|_1$	1.00	3.25
$\|\mathbf{u}\|_0$	2.01	3.92
$\|p\|_0$	1.65	2.14

Table 1: Convergence rate of the element-size h for the Mini element. Note that for small ϵ we get two orders faster convergence than the standard error estimates.

Figure 5 and Table 1 present the results for the Mini element applied to our Stokes problem (1)-(3). For $\epsilon = 1$, Table 1 confirms the standard error estimates for the velocity. For small ϵ we get two orders of convergence higher than predicted by the standard error estimates.

From Figure 5, we notice that for not too small values of ϵ, the error of the velocity converges linearly with respect to ϵ. For a given value of ϵ (dependent of the element size h), this linear dependency stops, due to the domination of the error term $h^3\|\epsilon\mathbf{f} + \nabla g\|_0$. But we notice the increased order of convergence with respect to the element size h, as also stated in Table 1. The pressure shows no clear signs of improved convergence, as we will expect. We do get a region where the error of the pressure converges linearly with respect to ϵ. However, this is up to the point where $\epsilon\mathbf{f} \approx \nabla g$.

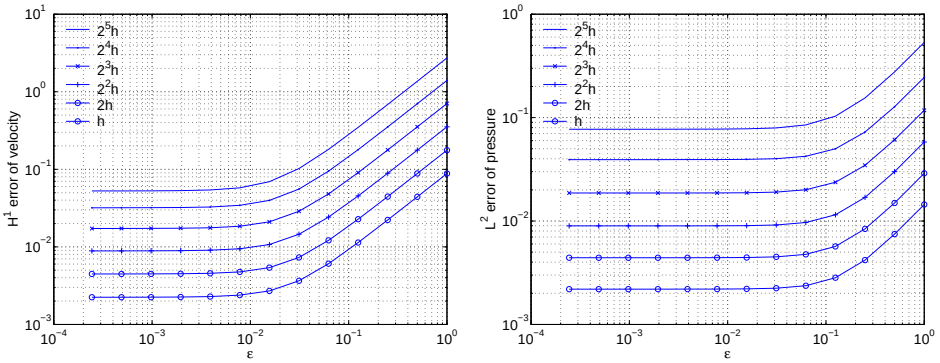

(a) H^1 error of the velocity

(b) L^2 error of the pressure

Fig. 6: The Crouzeix-Raviart element applied to (1)-(3). Convergence results are listed in Table 2. The convergence with respect to ϵ is only true until $\epsilon\mathbf{f}$ is of the order of ∇g. This region of convergence is therefore not dependent of the element size h. We do not experience an increase in the order of convergence with respect to h for small values of ϵ. Obviously the Mini element is superior to the Crouzeix-Raviart element for this type of problems.

	$\epsilon = 1$	$\epsilon = 2 \cdot 10^{-4}$
$\|\mathbf{u}\|_1$	0.99	0.86
$\|\mathbf{u}\|_0$	1.94	1.74
$\|p\|_0$	1.07	1.03

Table 2: Convergence rate of the element-size h for the Crouzeix-Raviart element.

The Crouzeix-Raviart element, as shown in Figure 6 and Table 2, shows no sign of increased approximation properties compared to the standard error estimates. This is probably due to the fact that Crouzeix-Raviart does not satisfy the weak inf-sup condition. We do have a small

region where the velocity error converges linearly with ϵ. But this region is small (approximately one decade instead of more than three decades for the Mini element), and it is not increasing when the element size is decreased. This small region of convergence is due to the fact that a reduction in $\epsilon\mathbf{f}$ will decrease the error until it is of the order of ∇g. Notice the difference; for the Crouzeix-Raviart element we have linear convergence with respect to ϵ until $\epsilon\mathbf{f} \approx \nabla g$, while for the Mini element we have the same convergence until $h\epsilon\|\mathbf{f}\|_0 \approx h^3\|\epsilon\mathbf{f} + \nabla g\|_0$. Obviously the Mini element is vastly superior to the Crouzeix-Raviart for this test-problem.

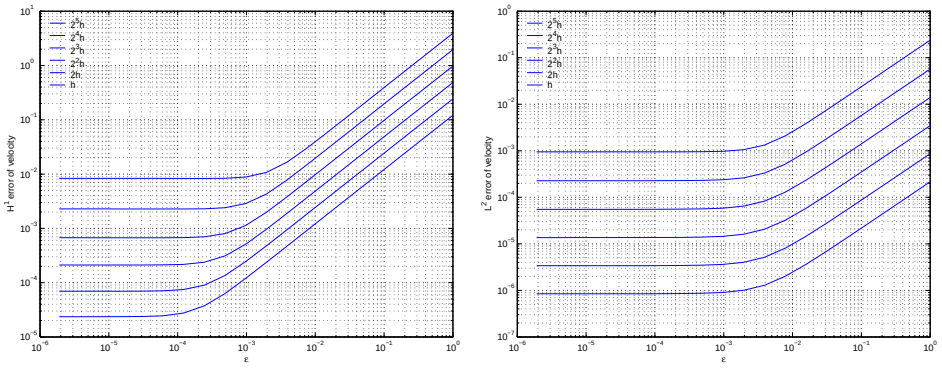

(a) H^1 error of the velocity

(b) L^2 error of the velocity

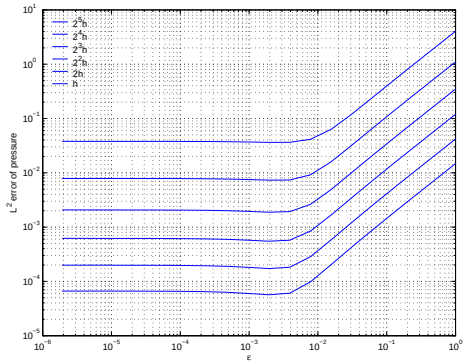

(c) L^2 error of the pressure

Fig. 7: Stabilized linear elements applied to (22). $\beta = \frac{1}{80}$. Convergence results are listed in Table 3. For the $\mathbf{H}^1$ error norm of the velocity, we note an increase in the region of convergence with respect to ϵ. This is even though the stabilization technique used is not stable for the mixed Poisson problem, and we would not expect to get an improved convergence for small ϵ. However, the $\mathbf{L}^2$ error norm of the velocity shows no sign of improved convergence. The reason for this different behavior is unknown to the authors. Still the stabilized linear element is considered better than the Crouzeix-Raviart element for these kind of problems.

The stabilized linear element in Figure 7 and Table 3 is presented for completeness, since different stabilization techniques are frequently used for the Stokes problem. This stabilization technique (with $\beta = \frac{1}{80}$) is considered to have equal properties as the Mini element for the Stokes problem. However, this is not so clear for the mixed Poisson problem. Therefore we cannot expect stabilized linear elements to have the same behavior as the Mini element. An interesting thing is the different behavior of the error of the velocity measured in the $\mathbf{H}^1$ norm compared to the $\mathbf{L}^2$ norm in Figure 7. The $\mathbf{H}^1$ error plot shows the typical behavior of an

	$\epsilon = 1$	$\epsilon = 2 \cdot 10^{-4}$
$\|\mathbf{u}\|_1$	1	1.77
$\|\mathbf{u}\|_0$	2	2
$\|p\|_0$	1.69	1.98

Table 3: Convergence rate of the element-size h for the stabilized linear element, with $\beta = \frac{1}{80}$.

element that satisfies the "weak" inf-sup condition. Note that the range of the linear convergence of ϵ is extended for smaller elements. We also have one order higher convergence with respect to the element size h for small values of ϵ. These signs are not present in the $\mathbf{L}^2$ error plots. Why this is the case is unknown to the authors.

NUMERICAL EXPERIMENTS ON THE STATIONARY INCOMPRESSIBLE NAVIER-STOKES EQUATIONS

We now consider a stationary Navier-Stokes problem

$$
\begin{aligned}
u \cdot \nabla u - \nu \Delta \mathbf{u} + \nabla p &= \nabla g + \epsilon \mathbf{f}, \quad \text{in } \Omega, && (26)\\
\nabla \cdot \mathbf{u} &= 0, \quad \text{in } \Omega, && (27)\\
\mathbf{u} &= \mathbf{u}_E, \quad \text{on } \partial\Omega_E, && (28)\\
\nu \frac{\partial \mathbf{u}}{\partial \mathbf{n}} - p \cdot \mathbf{n} &= g \cdot \mathbf{n} + \epsilon \mathbf{k} \quad \text{on } \partial\Omega_N, && (29)
\end{aligned}
$$

where $\mathbf{k}$ is a given function, $\partial\Omega_E$ is the part of the boundary with essential boundary conditions, and $\partial\Omega_N$ is the part with the natural boundary conditions. The constant $\frac{1}{\rho}$ is absorbed into the pressure variable p. It is easy to extend the splitting of the Stokes problem (1)-(3), done in a previous section, to the Navier-Stokes equations (26)-(29). The importance of the weak inf-sup condition is still true, meaning that Conjecture 1 is also true for the stationary Navier-Stokes equations. We will now test this using the Taylor-Hood element, which satisfy the weak inf-sup condition, and the $P_2 - P_0$ which does not.

Again we choose a simple example with the known analytical solution (22) which satisfies the model problem (26)-(29). Compared to (26) the right hand side will be

$$\epsilon \mathbf{f} + \nabla g = -\Delta \mathbf{u} + \nabla p + \mathbf{u} \cdot \nabla \mathbf{u}$$

One side of the domain has a natural boundary condition, while the others have essential boundary conditions. Again, by using (19), we predict that for small values of ϵ, the error from the approximation of the pressure may influence the error of the approximation of the velocity, depending of the choice of element.

As for the Mini element, we also work on extend the analysis of the error estimates for the Taylor-Hood element. Since this is not presented here, the results are presented as a Conjecture based on the numerical experiments.

Conjecture 2 *Assume that we want to solve* (1)-(2) *using the Taylor-Hood element. Then the error estimates can be expressed as*

$$
\begin{aligned}
\|\mathbf{u} - \mathbf{u}_h\|_1 &\leq C(h^2 \epsilon \|\mathbf{f}\|_0 + h^3 \|\epsilon \mathbf{f} + \nabla g\|_0) && (30)\\
\|\mathbf{u} - \mathbf{u}_h\|_0 &\leq C(h^3 \epsilon \|\mathbf{f}\|_0 + h^4 \|\epsilon \mathbf{f} + \nabla g\|_0) && (31)
\end{aligned}
$$

The Taylor-Hood element shows very similar behavior as the Mini element, and the general comments on Conjecture 1 do also apply here. For small values of ϵ, the Taylor-Hood element only gain one order of convergence with respect to the element size h, as for the Mini element the increase is two orders of convergence. This means that for small values of ϵ, the Mini

element and the Taylor-Hood element has the same order of convergence for the velocity with respect to the element size h.

Figure 8 and Table 4 the numerical experiments for the Taylor-Hood element on the stationary Navier-Stokes problem. We notice the improved convergence for small values of ϵ. For more specific comments, the reader should refer to the previous section where the Mini element is commented.

	$\epsilon = 1$	$\epsilon = 2 \cdot 10^{-6}$
$\|\mathbf{u}\|_1$	1.98	2.74
$\|\mathbf{u}\|_0$	2.98	3.86
$\|p\|_0$	3.00	2.00

Table 4: Convergence rate of the element-size h for the Taylor-Hood element. Note that for small values of ϵ we get one order higher convergence than the standard error estimate.

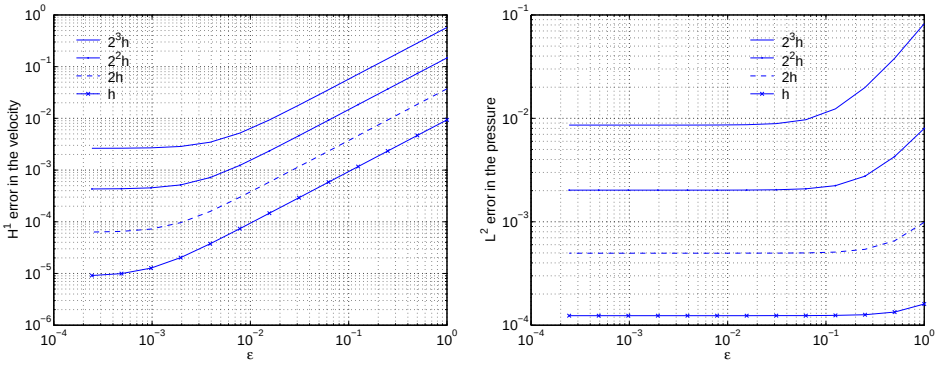

(a) H^1 error of the velocity

(b) L^2 error of the pressure

Fig. 8: The Taylor-Hood element, applied to (26)-(29). Convergence results are listed in Table 4. We notice the increase in the region of convergence with respect to ϵ, and the increased order of convergence for small values of ϵ.

	$\epsilon = 1$	$\epsilon = 2 \cdot 10^{-4}$
$\|\mathbf{u}\|_1$	1.87	0.91
$\|\mathbf{u}\|_0$	2.64	1.83
$\|p\|_0$	1.02	0.969

Table 5: Convergence rate of the element-size h for the $P_2 - P_0$ element. We notice that for small values of ϵ, we do not even get the expected convergence from the standard error estimate. This is because we have under-resolved the problem, and are therefore outside the asymptotic regime.

For the $P_2 - P_0$ element, Figure 9 and Table 5 indicate that we do not even get the standard error estimates for small values of ϵ. This is due to the poor approximation properties for these kind of problems. For the used number of elements, we are outside the region where we can expect the asymptotic convergence of the standard error estimates.

CONCLUSIONS

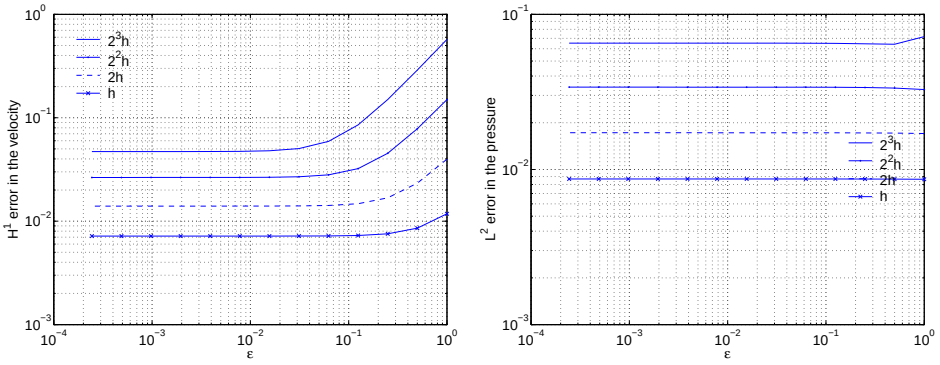

(a) H^1 error of the velocity

(b) L^2 error of the pressure

Fig. 9: The $P2 - P0$ element, applied to (26)-(29). Convergence results in the element-size h are listed in Table 4. There are no signs of improved convergence for small values of ϵ. This is as expected since the $P_2 - P_0$ does not satisfy the weak inf-sup condition.

In this paper we have focused on the use of some standard mixed elements applied to incompressible fluid flow. In particular we have focused on the case where the hydrostatic part of the pressure is dominating, and the pressure is large relative to the velocity. We have shown that elements like the Taylor-Hood and the Mini element handle this situation well, in contrast to the Crouzeix-Raviart and the $P_2 - P_0$ element. This seems to be related to the fact that the Taylor-Hood and the Mini element give stable approximations of the mixed Poisson problem. Finally, we have seen that these ideas apply to the stationary Navier-Stokes equations with general boundary conditions.

*

Acknowledgements The authors are grateful to Dr. A. Huerta, Professor H. P. Langtangen, and Professor R. Winther for many useful discussions.

REFERENCES

Arnold, D., Brezzi, F., and Fortin, M. (1984). A stable finite element method for the Stokes equations. *Calcolo*, 21:337–344.

Bacuta, C. and Bramble, J. (2003). Regularity estimates for solutions of the equations of linear elasticity in convex plane polygonal domain. *Math Phys.(ZAMP)*.

Bercovier, M. and Pironneau, O. (1979). Error estimates for finite element method solution of the Stokes problem in primitive variables. *Numer. Math*, 33:211–224.

Braess, D. (2001). *Finite Elements*. Cambrigde.

Brenner, S. and Scott, L. (1994). *The mathematical theory of finite element methods*. Springer Verlag.

Brezzi, F. and Fortin, M. (1991). *Mixed and hybrid finite element methods*. Springer Verlag.

Crouzeix and Raviart, P. (1973). Conforming and non–conforming finite element methods for solving the stationary Stokes equations. *RAIRO Anal. Numér*, 7:33–76.

Girault, V. and Raviar, P.-A. (1986). *Finite element methods for Navier-Stokes equations*. Springer Verlag.

Gresho, P. M. and Sani, R. L. (1998). *Incompressible flow and the finite element method*, volume 2. Wiley.

Gunzburger, M. D. (1989). *Finite Element Methods for Viscous Incompressible Flows – A Guide to Theory, Practice and Algorithms*. Academic Press.

Lin, C. and Segel, L. (1974). *Mathematics Applied to Deterministic Problems in Natural Sciences*. SIAM.

Mardal, K., Tai, X.-C., and Winther, R. (2002). A robust finite element method for Darcy–Stokes flow. *SIAM J. Numer. Anal.*, 40:1605–1631.

Mardal, K. and Winther, R. (2004). Uniform preconditioners for the time dependent Stokes problem. *Numer. Math.*, 98(2):305–327.

Quarteroni, A. and Valli, A. (1997). *Numerical Approximation of Partial Differential Equations*. Springer.

Rannacher, R. and Turek, S. (1992). A simple nonconforming quadrilateral Stokes element.

Turek, S. (1999). *Efficient Solvers for Incompressible Flow Problem*. Springer Verlag.